An Investigation into Range-Energy and Stopping Power
NE 427 - Range-Energy Lab Report 5

July 31, 2020

1 Abstract

Radiation dose occurs through the process of energy deposition from charged particles into matter. When working with nuclear materials, people are often exposed to radiation, which therefore requires shielding. To determine the effectiveness of the shield on the charged particles and gammas, quantities like the range and stopping power need to be observed and quantified. In this work, the range of α-particles and gamma rays, as well as the stopping power of materials like Aluminum and Lead was observed.To do this, the lab was split up into two weeks, with the first week focusing on the alphas while the second week focused on the gammas. The first week involved using a pressurized canister to model changing thicknesses of some absorber to determine the range of the α-particles. From this process the range of the alphas were experimentally determined to be 4.517 cm, which was very close to the known extrapolated distance of alphas which is 4.051 cm. The second week involved using various slabs of lead and aluminum to gather spectra and observe the attenuation of the gammas through the materials. The data obtained from this experiment seemed off given the large variance from the known NIST values. Overall, the lab provided an excellent insight into the the ideas of range and stopping power, and how different materials and different charged particles have different respective properties.

Contents

1 Abstract **1**

2 Introduction and Background **3**

3 Approaches and Methods **5**

4 Results and Analysis **8**
4.1 Week 1 Results and Analysis 8
4.2 Week 2 Results and Analysis 12

5 Discussion of Results **16**
5.1 Week 1 Discussion 16
5.2 Week 2 Discussion 16

6 References **18**

2 Introduction and Background

Energy interaction and deposition into matter is a very important topic for nuclear engineering related topics. Individuals exposed to radiation emitting materials receive a dose that is dependent on the particle's incident energy or specific parts of an individual's body, which can lead to potential adverse complications. Depending on the individual's absorbed dose, afflictions such as DNA strand breaks and other stochastic adverse effects may occur. Therefore, it is important to investigate and understand how energy and charged particles interact with matter, in particular how radiation is absorbed.

The first week of lab revolved around detecting alphas and their ability to travel through an absorber. Given that the goal the first week was to test varying thicknesses of some arbitrary absorber, but that physically it can be very difficult to have a homogeneous material and uniform intervals, a pressurized gas chamber was used instead. Therefore the pressure in the chamber was altered to observe to notable quantities for the detection and measurement of energy deposition into matter.

Two of the key quantities to understand when conducting experiments based around the deposition of energy into matter are the stopping power and the range. The stopping power of a material describes the energy loss of charged particles traveling through a given medium, in particular, the medium's ability to reduce a charged particle's energy. This quantity can also be defined mathematically in a couple different ways given that there exists both the classical form and the Bethe stopping power, however in its most general form, the stopping power is mathematically written as

$$S(E) = -\frac{dE}{dx} \tag{1}$$

To build off of the stopping power, the range is defined as the amount of distance a charged particle can travel through a material or substance before ultimately having zero energy. Mathematically, this quantity can be derived from the magnitude of the stopping power, specifically by integrating up to the incident particle energy E_0 such that

$$R = \int_0^{E_0} \frac{dE}{\left|-\frac{dE}{dx}\right|} \tag{2}$$

It should be noted that the range is not necessarily a suitable model for light charged particles such as electrons or positrons, though this is not as relevant for the experiment being conducted. On a more physical level, the range is the distance in which charged particles, such as α particles, can travel before the initial number of them drops to 50% of the original value.

The stopping power and range are important measures that are dependent on a number of different conditions. For example, α particles have a range is quite small as seen by the fact that a thin sheet of paper is able to stop the alphas very easily. That is not to say that paper has a large stopping power, but rather that the range of alpha particles is shorter than the thickness of a sheet of paper. In contrast, γ rays are far more penetrating and require a material with a large stopping power in order to effectively be shielded. While the first week's lab focused more on the alpha range than actual shielding, it is worth making the connection that these calculations are a very important step in developing effective shields.

The second week of lab focused on gamma interaction with matter and the attenuation of gamma radiation. Depending on the energy of the incident gammas and the Z of the absorber, three different types of interaction are possible: the photoelectric effect, Compton scattering and Pair Production. To determine the linear attenuation coefficient μ, the contributions of the interactions of each case all need to be summed in order to determine the total attenuation coefficient. In this case, Rayleigh scattering can be ignored due to the fact that there is no net energy transfer in a Rayleigh scattering event, and it is assume that nuclear pair production and triplet production can be collected into one "pair production" term. Thus the attenuation coefficient can be determined to be

$$\mu = \mu_{PE} + \mu_C + \mu_{PP} \tag{3}$$

or

$$\mu = \sigma_{PE} 2n + \sigma_C n_e + \sigma_{PP} n$$

where n is the density of the nuclei, and n_e is the electron density. However, it should be noted that with varying forms of a similar material, there may be different attenuation coefficients. Therefore, it is beneficial to define a second quantity, the mass attenuation coefficient. This quantity is easily found as it is just the linear attenuation coefficient divided by the density of the material through which it travels. For example, consider liquid water, vapor and ice. Each substance has the same chemical structure, however all three have different material properties and different densities, thus is is important to have a more general term, hence the need for a mass attenuation coefficient.

In contrast to α-particles, gamma rays are able to penetrate through much thicker materials but their paths may not always be uniform. Given that the gamma interaction in matter is essentially a stochastic process, it helps to define another key term, the mean free path. As the name implies, the mean free path is the distance in which a gamma can ravel through an absorber before interaction. In general, this quantity is just the reciprocal of the linear attenuation coefficient, though it can also be determined mathematically from the Beer Lambert Law for the counting rate with an absorber $I = I_0 e^{-\mu t}$ (where I_0 is the count rate without an absorber, t is the absorber thickness and μ is the linear attenuation coefficient of the absorber). Given that this is technically an average, or an expectation (these are used interchangeably here even though technically they are slightly different), we can express this mathematically as

$$\langle x \rangle = \lambda = \frac{\int_0^\infty x e^{-\mu x} dx}{\int_0^\infty e^{-\mu x} dx} = \frac{1}{\mu}$$

The mean free path is also quite relevant in dose calculations as it allows for researchers to determine how much energy the incident gammas may have prior to interacting with the absorber, and how much dose an individual, like a patient, may receive. The mean free path can also be used to deduce how thick an absorber is in terms of mean free paths, with one mean free path being the distance in which approximately 37% or 1/e of the incident photons are attenuated.

3 Approaches and Methods

The lab portion of this experiment was broken up into two separate weeks, each focusing on a different type of emission. In the first week, the range of alpha particles was measured, while in the second the lab instead focused on the attenuation of gamma radiation.

The first week used Americium-241 (^{241}Am) as an alpha emitter in conjunction with a silicon-diffused junction detector mounted inside of a vacuum canister. As seen in Figure 1 below, the Americium was placed inside of a vacuum chamber with a detector directly above it which was connected to a detector bias supply.

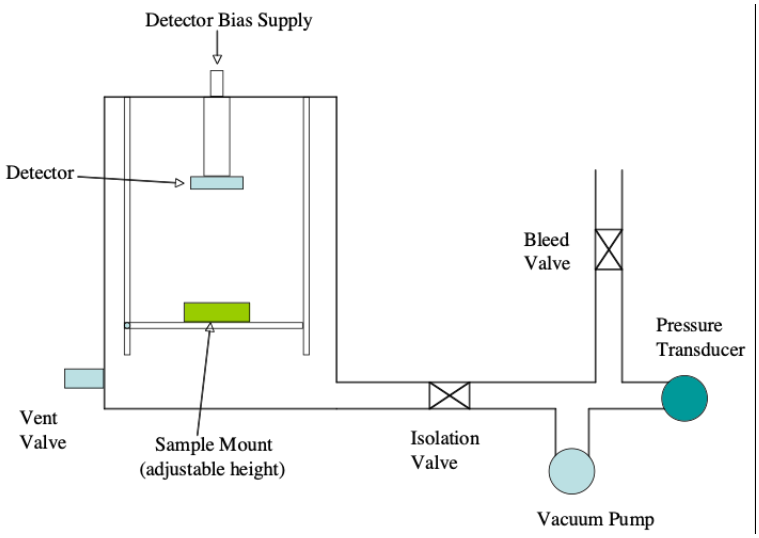

Figure 1: The schematic of the setup for the first week experiment

The alphas traveled through the chamber to the detector in an attempt to model alpha traveling through an absorber. To simulate altering the thickness of the "absorber", the pressure in the canister was increased and decreased as needed by adjusting the applied voltage of the system. In particular, the pressure-thickness relationship was given by

$$d_{eff} = \frac{1}{\rho_{STP}} \frac{P(MW)_{air}}{RT} d \tag{4}$$

where d_{eff} was the effective thickness, ρ_{STP} was the density at standard temperature and pressure, MW was the molecular weight, RT was the product of the gas constant and temperature, and d was the sample-detector distance. The relationship between the pressure and voltage was linear which was seen by increasing the voltage from 4.5 mV to 5150 mV , the pressure also increased from 0.46 Torr (or millimeters of Mercury) to 526.07 Torr. This relationship was determined by first finding the corresponding voltage for when the pressure in the canister was approximately 760 Torr. The voltage at this point was recorded, and then a linear relationship was determined. In this lab's case the determined voltage was found to be approximately 7.44±0.01 V, and this value was divided by the applied voltage, and it was assumed that at zero voltage, the pressure would also be zero. Therefore, the voltage-pressure relationship was determined to be:

$$Pressure = (Voltage \pm 0.01) \times \left(\frac{760 Torr}{7.44 \pm 0.01 V} \right) \tag{5}$$

To account for the slight error in the voltage, a small error analysis can be done to determine the error on the pressure. Note that the error on $\left(\frac{760 Torr}{7.44 \pm 0.01 V}\right)$ is 0.001344 Torr/V

$$\frac{\sigma_P}{P} = \sqrt{\left(\frac{0.01}{Voltage}\right)^2 + \left(\frac{0.001344}{102.151}\right)^2}$$

Therefore this error is dependent on the applied voltage in each case. This process allows for the relationship between the pressure and the voltage to be seen, and ultimately created a model for the thickness of some absorber.

From this setup, after the source was inserted, a few more steps were taken in order to adequately generate spectra. Through the setup with the amplifier, as shown in figure 2, the detector was connected to a pre-amplifier in order to get a view on an oscilloscope to verify that counts were being detected.

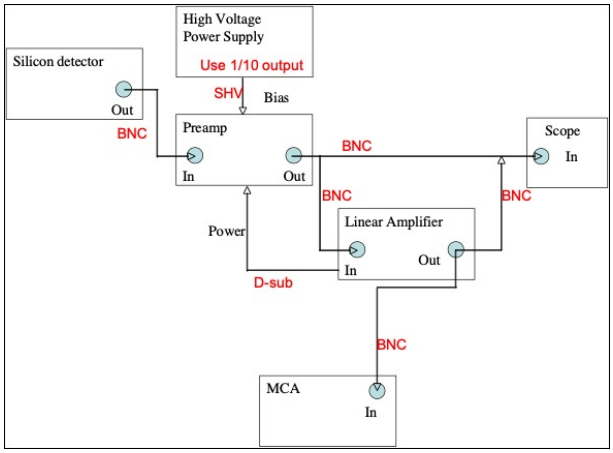

Figure 2: The electronic schematic of the setup from the first week of lab.

In this case, there was an applied voltage of approximately 0.032 kV or 32 V. From this and the fact that the scope trace was observed to be 1 volt per division, the pulse height was found to be approximately 4V. This peak height was generated from the pre-amp having a coarse gain at 50 and a fine gain at 13.2, with a shaping time of $0.5\mu s$. Therefore it was determined as well that the initial pressure in the chamber, and the first reading that was taken was at 0.46 Torr. Additionally, in the set up, the distance between the alpha source and the sodium detector was measured to be 6 cm. This was the set up for the first week of lab.

For the second week of lab, a similar circuit setup was used, but a much different detection process was used. For the detection of gammaes, Gold-198 was loaded into a lead pig and was then surrounded by lead collinators to ensure the gammas travelled in the correct direction, specifically towards the NaI(TI) detector, as seen in Figure 3.

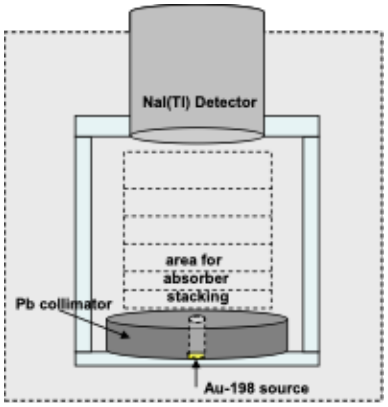

Figure 3: The schematic of the lab setup for the second week.

From this setup, slabs of lead and/or aluminum were placed atop the source in order to observe the gamma spectrum with he given absorbers. Additionally, a plus was also placed atop the source in order to observe any possible background data, and this reading was done in conjunction with the "unplugged" testing. Throughout the testing, a 1kV voltage was applied in order to make sure that counts were being detected which, like before, was observed on the oscilloscope. On the oscilloscope, similar volts per division and shaping time were used, however the pre-amp had a total gain of 20 in this case.

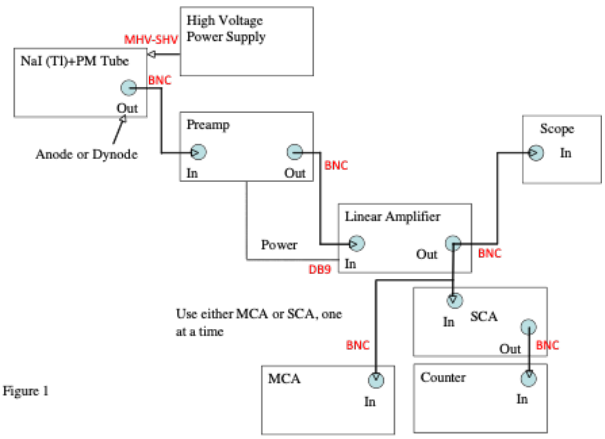

Figure 4: Contrary to the small text saying this is "figure 1", this is the electronic schematic of the lab for week 2.

Before beginning to generate spectra in Quantum Gold, the system had to first be calibrated. This was done by first generating a spectrum of ^{198}Au without any absorber and observing where the photopeak appeared. This will be covered in more detail in the results and analysis sections, but in general the photopeak appeared across the range of energy bins 341 to 435 for the case when the total number of bins or channel was 1024. Furthermore, the full-width half-max of the photopeak was found to be exactly 71.00, meaning that the peak was considerably broad. This process provided a control-esque data spectrum, which was used to compare the other spectra as a result.

4 Results and Analysis

The results section will be broken into two sections in order to account for both weeks as for ease of understanding.

4.1 Week 1 Results and Analysis

The data recorded in the first week of the lab, specifically the measured applied voltage, the resulting total counts, and the other calculated columns are found in Table 1 below.

Table 1: The Center of Peak Channel Data gathered from varying Applied Voltage

Voltage [mV]	Pressure [Torr]	FWHM	Total Counts	Peak Channel	Energy [MeV]
4.5	0.459675	4.14	1199	448	4.375
113	11.54295	3.44	753	443	4.32617
500	51.075	6.7	1235	421	4.11133
1000	102.15	8.84	1153	401	3.91602
1510	154.2465	13.71	1109	364	3.55469
3000	306.45	15.91	1069	265	2.58789
4490	458.6535	39.78	1151	134	1.30859
5000	510.75	47.33	1169	69	0.67383
5150	526.0725	52.67	1147	49	0.47852
5350	546.5025	34.58	744	24	0.23438
5500	561.825	5.6	65	10	0.18555

The pressure for each applied voltage was calculated by multiplying the applied voltage by the conversion factor of 102.15 and then divided by 1000 to convert into Torr or millimeters of mercury. The Full-Width Half-Max,Total Counts and Peak Channel values were gathered directly from the spectrum gathered in Quantum Gold and the Energy corresponding to the center of the peak was calculated by using the conversion which has been used and justified in previous lab experiments:

$$Energy = \frac{ChannelNumber}{1024 Channel/MeV} \times 10 \tag{6}$$

From these readings, spectra were also obtained. Individually, each spectrum had very obvious peaks that shifted down the channel range from around channel 448 to around channel 10 by the end of the testing. The peak also widened considerably and thus the resolution of the peak was noticeably lower, as seen by the column detailing the FWHM increasing further along the table. Below are a few of the plotted spectra for the different tested voltages (and therefore tested pressures).

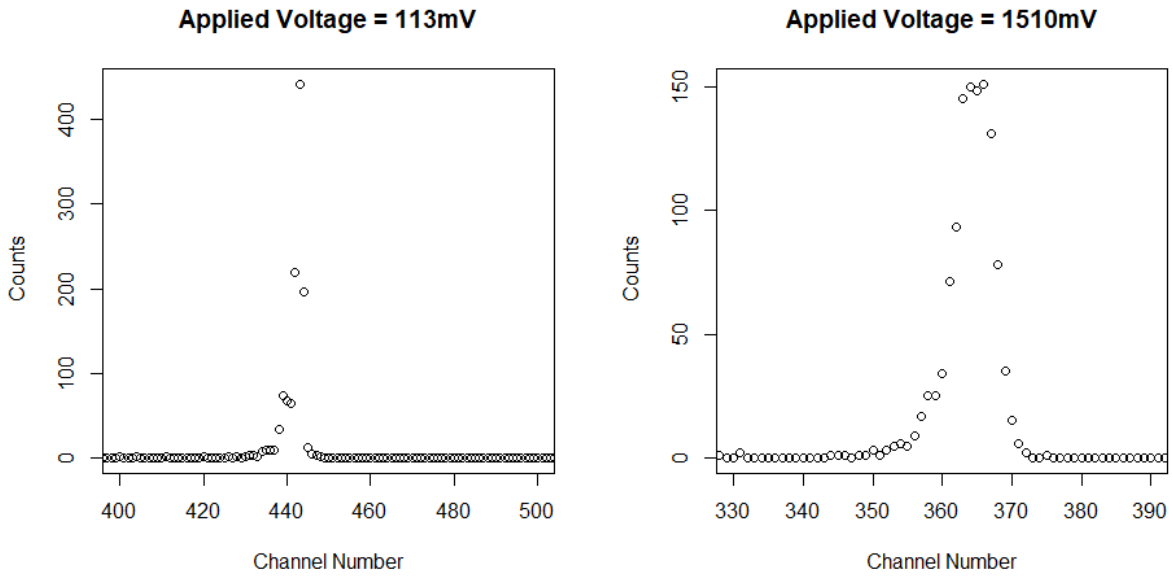

Figure 5: The spectrum peak for when 113mV and 1510mV were applied

To better visualize this trend, six different pressure's spectra were plotted on the same graph as shown below.

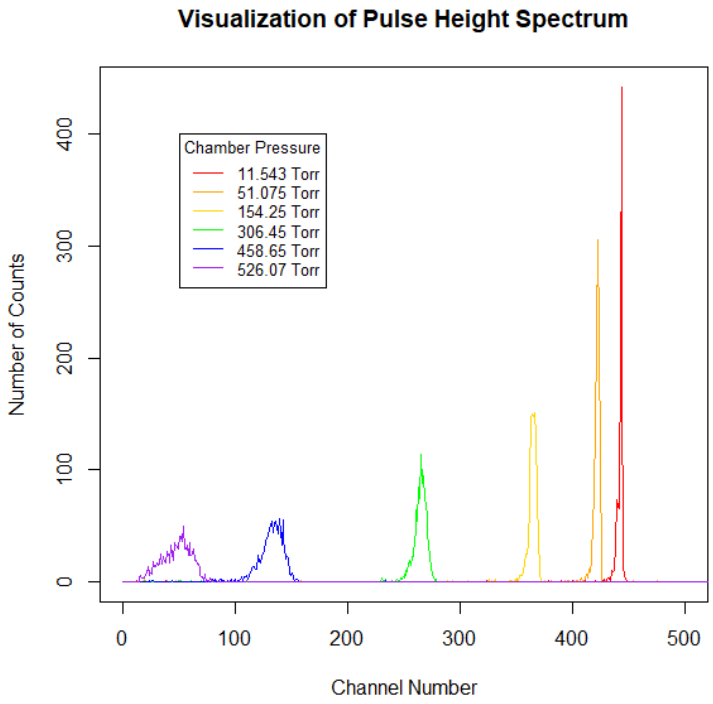

Figure 6: Six different pressures plotted on the same graph

As inferred by the table, the spectrum peaks plotted on the graph show a couple notable trends. As seen previously, the peaks appear to widen and get shorter as the pressure increases.

This data also allows for a determination of the most probable energy for a given absorber thickness. In particular this value can be determined by creating a spline over the data points that were used, in order to visualize the relationship. Assuming an error of approximately 2 Torr, and a channel error of 1, the following plot can be generated appropriately.

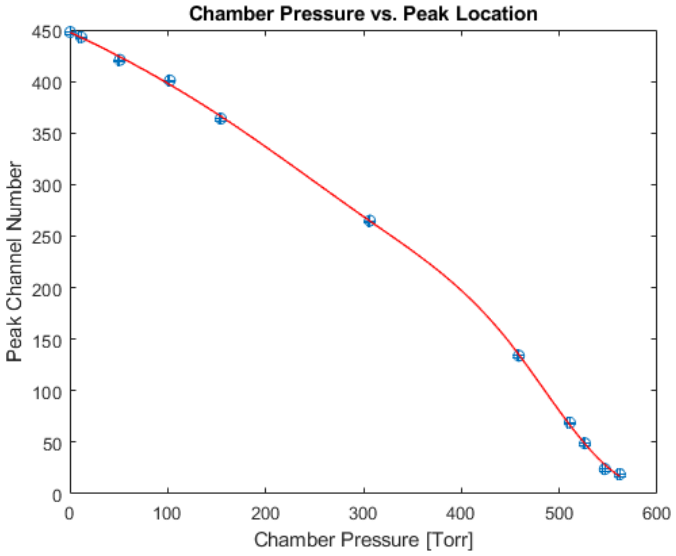

Figure 7: A plot of the spline (with DoF 4) fit of the Peak Location as a function of chamber pressure

It is also beneficial to plot the change in the full-width half-max as a function of chamber pressure as well.

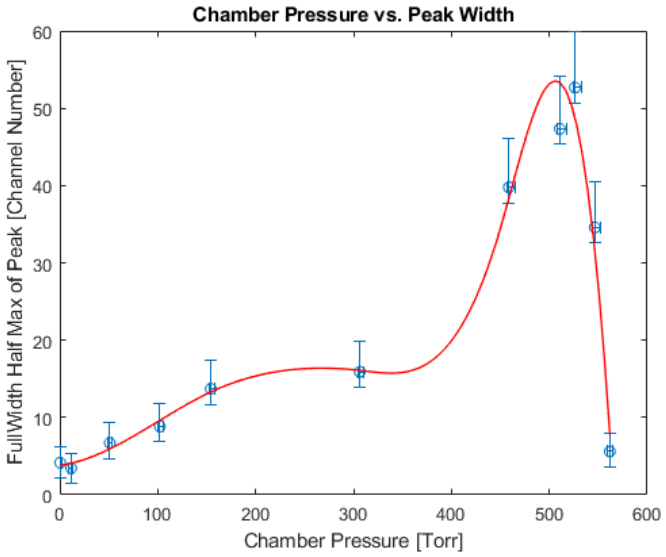

Figure 8: A plot of the spline (with DoF 4) fit of the FWHM as a function of chamber pressure

The mean energy in this case for the alphas can also be observed from calculating the effective distance in the absorber for each respective pressure. To do so, the effective distance as shown in equation 4 needs to be used with the following constant values:

$$d_{eff} = \frac{(6cm)}{1.2mg/cm^3} \frac{P \times 133.32}{\frac{(8.314\frac{J}{K \cdot mol})(293K)}{0.02897kg/mol}} \tag{7}$$

To generate a distance for each corresponding pressure value. After applying this transformation, the next plot can be made to show the relationship between the mean energy and the effective distance.

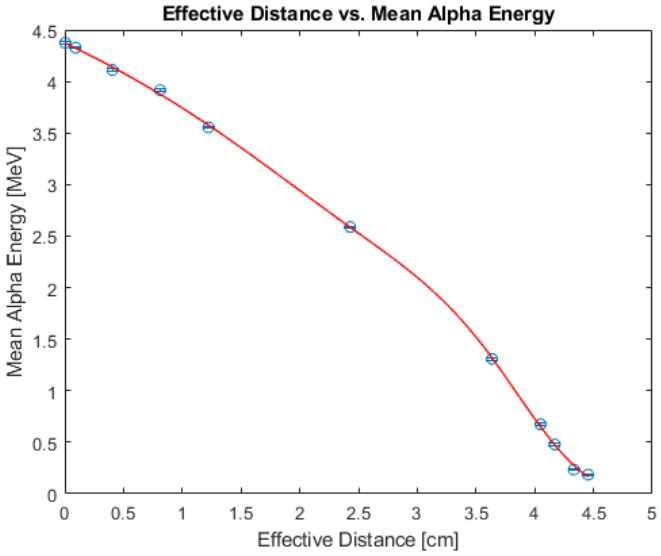

Figure 9: The mean energy as a function of effective distance of the absorber (Spline with DoF 4)

This plot does look very similar to the plot for the Chamber Pressure vs. Peak Location, which intuitively makes sense. As a sanity check, it can be seen that the two values plotted in Figure 9 are both derived from the two quantities in Figure 7 by a linear transformation. Therefore the shape of the plot should not change at all from one plot to the next, even if the quantities on each of the axes do.

The mean stopping power can also be determined for each pressure based off of the data. This process can be done by taking the difference between each mean energy value and the difference between each of the effective distances and then dividing the latter by the former such that

$$\left\langle -\frac{dE}{dx} \right\rangle = \frac{\Delta E_\alpha}{\Delta d_{eff}} \tag{8}$$

This is easily done from generating more calculated columns in Table 1. This therefore allows for a quick creation of the plot for the stopping power as a function of mean alpha energy.

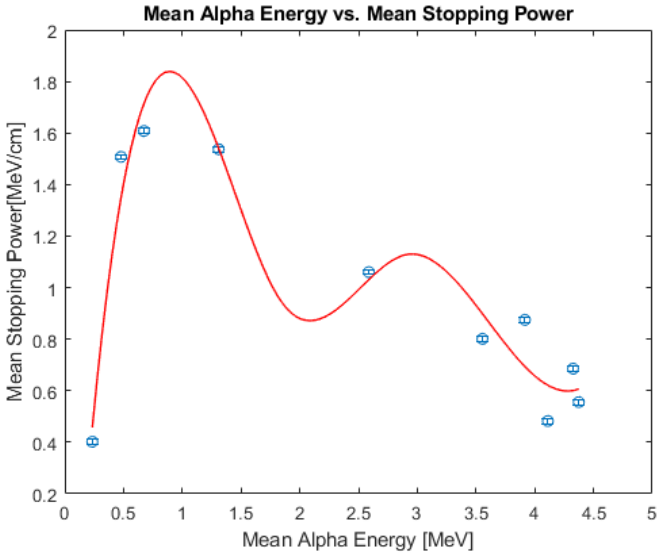

Figure 10: The stopping power as a function of Mean alpha energy (Spline with DoF 4)

Given that the tests were taken for two minutes (120 seconds), a counting curve can also be generated. To do so, all that needs to be done is to make yet another calculated column from the total number of counts for each given pressure and divide the value by 120 seconds. The error for this part as well is assumed to just be a square root of the counts in order to have reasonably small values. Therefore, a counting curve based on effective distance can be generated as shown in figure 11 below.

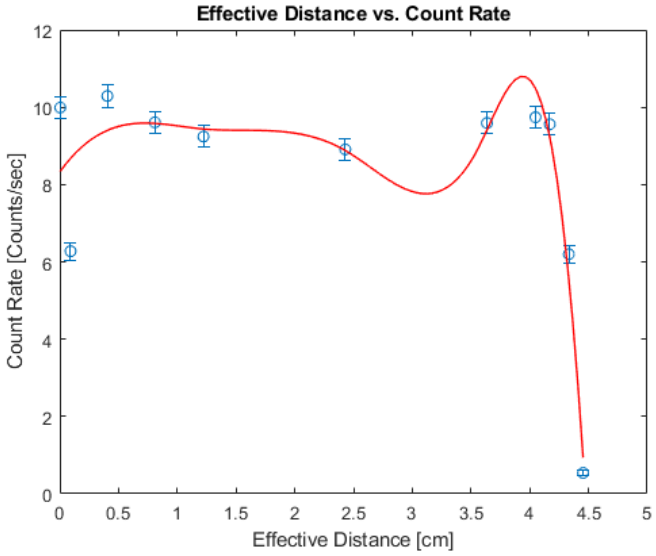

Figure 11: The counting curve for the alpha particles as a function of the effective distance (Spline with DoF 4)

Note that in this case the extrapolated distance or Range for this setup is where the spline would cross the x-axis or equal zero. Also form this plot one can see something that may appear similar to a Bragg peak with a slight increase in energy before a drop-off.

4.2 Week 2 Results and Analysis

During the second week, a variety of spectra were obtained to observe how the thickness of the two absorbers tested (Aluminum and Lead) impacted the attenuation of gammas. Doing so yielded a couple different plots each one characterizing the differences between each setup. With the Gold-198 source, the combinations included using a lead absorber, an aluminum absorber, a plugged lead absorber and a plugged aluminum absorber. As noted previously, the plug acted as a way to observe background counts on each experimental set up in order to eventually remove any noise. The spectra are show below, and spectra of similar energies were chosen.

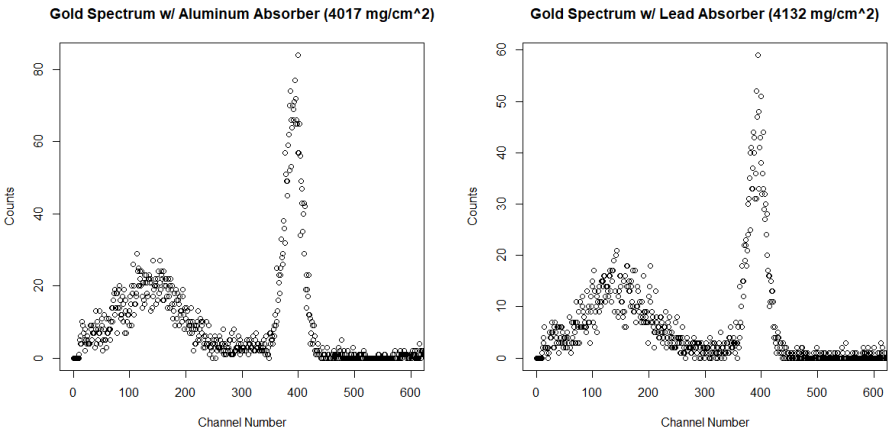

Figure 12: The spectra of Gold-198 with Aluminum and Lead absorbers with background counts

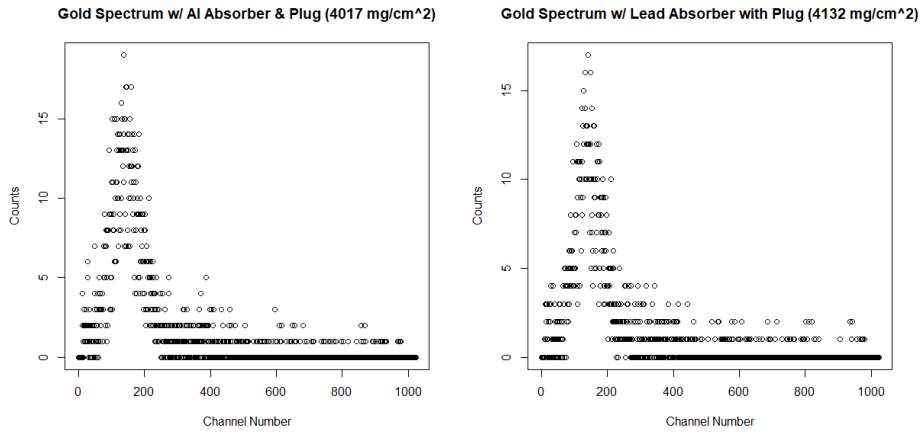

Figure 13: The spectra of Gold-198 with Aluminum and Lead absorbers background counts

To remove the excess noise, or background counts, the values of these two spectra were subtracted from one another. Thus the plots without any of the background counts are shown below in Figure 14.

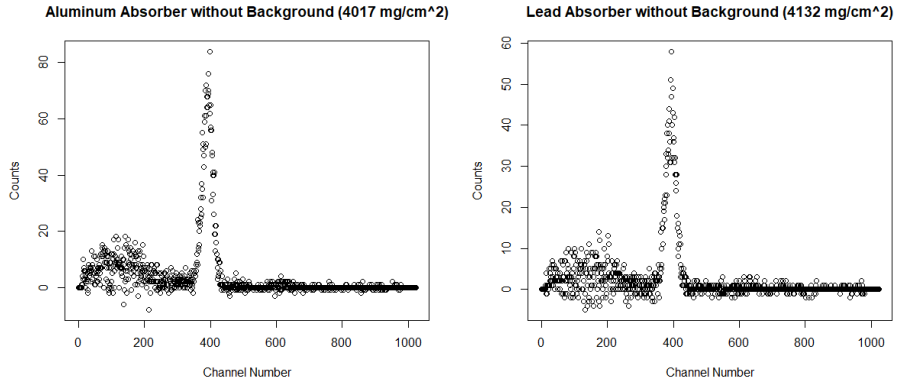

Figure 14: The spectra of Gold-198 with Aluminum and Lead absorbers accounting for background noise

It should be noted that for the aluminum, the peak channel number was 391, and the peak spanned channels 341 to 435, and the lead absorber was calibrated to be around the same range. Furthermore, the measured FWHM of each peaks was 77 and 73.5 respectively. Tables for the results of the two different absorbers, aluminum and lead, are given in tables 2 and 3 respectively below.

Table 2: The Number of Counts Based Aluminum Thickness

Thickness [mg/cm^2]	Counts without Plug	Counts with Plug
0	3600	0
141	3836	62
216	3581	51
616	3484	120
1041	3294	112
1988	2978	117
2961	2812	140
4017	2565	81
5194	2172	93
6150	2120	31
7279	2106	22
8239	1642	44
9452.5	1447	81
10083.8	1326	77

Table 3: The Number of Counts Based Lead Thickness

Thickness [mg/cm^2]	Counts without Plug	Counts with Plug
1120	2857	0
2066	2207	95
3448	1602	100
4132	1675	0
5514	1135	0
6634	917	19
7367	886	17
8487	696	55
9433	331	0
10815	323	0

In order to determine the linear attenuation coefficients of these two systems, a fitted line process must be used. However, the workflow for this is outlined in the "Curve fitting example" document found on the course CANVAS page. Therefore, the plots and their fitted line equations are shown below. Furthermore, the fitted line equations are also given which allows for the discovery of the linear attenuation coefficient. Below are the plots that show the counts and the background counts, as well as the fitted lines for Aluminum and Lead.

For Aluminum,

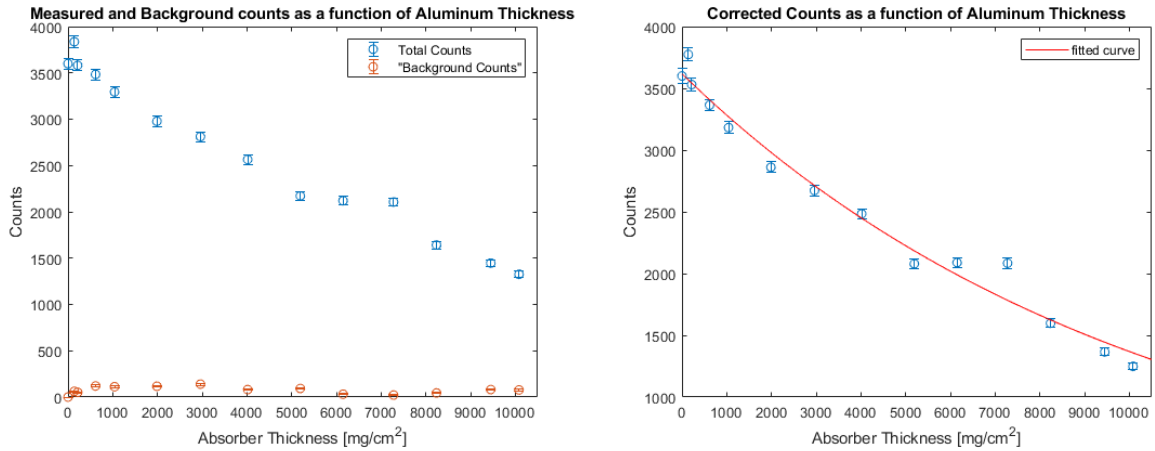

Figure 15: The Measured Data and Background Counts, and the Corrected Counts plot with a fitted exponential line for Aluminum

From the process of the curve fitting example, the fitted line shown in the right image has the equation is $y = 3618e^{-9.716\times10^{-5}x}$, where x is the absorber thickness and y is the number of Counts. Therefore the linear attenuation coefficient is found to be $9.716 \times 10^{-5} \pm 1.034 \times 10^{-5} \frac{1}{cm}$. To determine the mass attenuation coefficient, this value is just divided by the density of Aluminum such that:

$$\frac{\mu_{Al}}{\rho} = \frac{9.716 \times 10^{-5} \frac{1}{cm}}{2.7 \frac{g}{cm^3}} = 3.5986 \times 10^{-5} \frac{cm^2}{g}$$

For Lead, a similar process is conducted.

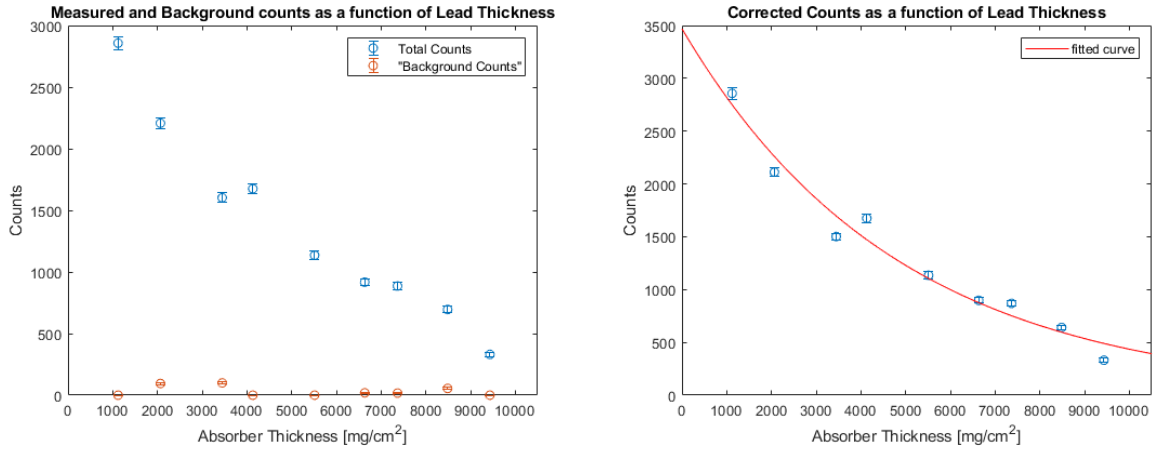

Figure 16: The Measured Data and Background Counts, and the Corrected Counts plot with a fitted exponential line for Lead

From the process of the curve fitting example, the fitted line shown in the right image the has equation $y = 3469e^{-2.075\times10^{-4}x}$, where x is the absorber thickness and y is the number of Counts. Therefore the linear attenuation coefficient is found to be $2.075\times10^{-4}\pm3.37\times10^{-5}\,\frac{1}{cm}$. To determine the mass attenuation coefficient for Lead, this value is just divided by the density of Lead such that:

$$\frac{\mu_{Pb}}{\rho} = \frac{2.075\times10^{-4}\,\frac{1}{cm}}{11.342\,\frac{g}{cm^3}} = 1.8292\times10^{-5}\,\frac{cm^2}{g}$$

5 Discussion of Results

5.1 Week 1 Discussion

One of the most prominent trends in modelling the alphas with a pseudo-absorber is the change in the peak shape as pressure is increased. As noted in the previous section, the peak shape begins with a very narrow and precise shape, and as pressure increases the shape of the peak changes. In particular, the peak height decreases and the peak shape becomes far more broad as seen in figure 6. The widening of the peak can pretty easily be seen by observing not only the overall shape of the peak, but also the range of channel numbers accounted for on the x-axis. Additionally, the counts observed on each spectra also appears to decrease with an increased in applied voltage. This fact makes intuitive sense as well given that the increase of applied voltage is meant to simulate increasing the thickness of an absorber, naturally causing less alphas to penetrate and be detected.

However, this trend also leads to a pretty significant question: "If no particles are stopped or lost, the area under a given peak should be constant. Why do the peak shapes change? " This is what happens to be a phenomenon called "Energy straggling", and it appears in this experimental setup because of the broadening of the peaks. Energy straggling is the process in which alphas traveling through an absorber and slowing down via a number of collisions, therein creating an energy loss distribution curve. When there is a higher pressure, or modelled higher thickness of an absorber, it is more likely that the alphas will have more collisions and less will penetrate enough to be detected, and that those that do will have a wide variety of energy values. Therefore, there will be a more broad detected and displayed energies, which is reflected in the peaks at higher pressures.

The extrapolated distance or range of the alpha particles can also be generated from the data obtained. AS previously noted below figure 11, the value of the extrapolated distance is simply where the spline equals zero. To generate the equation for another modelling curve, a sixth-order polynomial was generated in excel. This curve was found to be $y = -0.7956x^6 + 9.3391x^5 - 40.032x^4 + 76.481x^3 - 64.582x^2 + 22.025x + 31.047$. Solving this equation for when $y = 0$,likely on the interval [0,5] cm, reveals that the extrapolated distance for the tested setup is approximately 4.517cm. Compared to the known value of the extrapolated alpha distance of 4.051cm, this value is reassuringly close. there may be differences mainly due to the fact that lab experiment was not actually using absorbers, but rather using the pressure of a canister which could lead to some bit of variance.

5.2 Week 2 Discussion

As previously noted, the determined mass attenuation coefficients for Alumnium and lead were determined to be $3.5986 \times 10^{-5} \frac{cm^2}{g}$ and $1.8292 \times 10^{-5} \frac{cm^2}{g}$ respectively. A linear interpolation of the NIST Tables tables is done to determine the mass attenuation coefficients for Aluminum and Lead for incident gamma energies at 0.4118 MeV.

$$\left(\frac{\mu}{\rho}\right)_{NIST,Al} = 0.03106 + (.4118 - .4)\frac{0.02836 - 0.03106}{0.5 - 0.4} = 0.03074\frac{cm^2}{g}$$

(1)

$$\left(\frac{\mu}{\rho}\right)_{NIST,Pb} = 0.2323 + (0.4118 - 0.4)\frac{0.1614 - 0.2323}{0.5 - 0.4} = 0.2239\frac{cm^2}{g}$$

(2)

From this reference data, the values that were determined in the lab were significantly lower than expected. This may be the case because of the lab conditions as a whole given that the sources might not have had as high of an energy as expected.

The second week's lab used collimator in the lab setup for the week. A collimator is a small device that produces parallel beams of radiation which therefore allows for a rather "direct" line of gammas travelling in a certain director. In this case, a collimator was used in order to make sure that the gammas travelled through the placed absorbers in order to reach the detector without having the gammas that did not penetrate through the absorbers be detected. This, however, does lead to a problem with the experiment, namely the fact that background counts were observed even with he proper means of preventing them. This collimator device did work well, but it may have had some mechanical error which also may have contributed to the large discrepancy in the determined mass attenuation coefficients.

One of the issues with this week's lab is that there was always a slight error when obtaining counts as there were always some level of background counts. This of course stems from the fact that the source was never

actually removed from the pig when testing for the background, rather it was covered by a pin. The pin was effective and preventing most of the gammas from penetrating and being detected, however there were still some unavoidable counts being seen while the source was still in the lead pig. This issue could have easily been fixed had the source been consistently removed and inserted when looking for background values, however given lab policy, this would have made things take far longer and be more tedious than they needed to be. So in this case, while it did create some extra background noise, ultimately the background counts were minimal enough where reasonable analysis could still be conducted.

Overall this lab experiment provided an excellent visualization and understand of the range, stopping energy and gamma attenuation in matter. From the alpha energy side of the experiment, the extrapolated distance was determined to be 4.517cm, which was very close to the given distance for when the initial energy of the alpha was 5.486 MeV with a pressure at 760 Torr. The second week involved using gamma and observing the shielding ability of lead and aluminum. The results obtained from the lab seem to be much lower than the actual determined values from NIST however, which is unfortunate. In the end, the general processes of observing the range of charged particles and stopping power of certain materials was observed.

6 References

1. “X-Ray Mass Attenuation Coefficients - Aluminum.” NIST, physics.nist.gov/PhysRefData/XrayMassCoef/-ElemTab/z13.html.

2. “X-Ray Mass Attenuation Coefficients - Lead.” NIST, physics.nist.gov/PhysRefData/XrayMassCoef/-ElemTab/z82.html.

This report was written by Peter Hotvedt. His Lab partners were Mazna Aljneibi and Colin Swee.